DYNAMIC P-Δ EFFECTS OF RC COLUMNS

Hyo-Gyoung Kwak[1] , Jin-Kook Kim[2]

ABSTRACT

The purpose of this study is to investigate the dynamic P-Δ effect in reinforced concrete (RC) columns on the basis of the layered section method. In order to effectively analyze the cyclic behavior of RC columns which show the changes in the load-displacement relation according to the magnitude of axial load applied, the layered section approach is adopted, and a procedure to indirectly implement the bond-slip effect into the stress-strain relation of the reinforcing steel is used. To verify the validity of the method and to identify the significance of various effects on the global response of slender RC columns, nonlinear dynamic analyses are conducted for sixty sets of horizontal and vertical earthquakes with practical ranges of slenderness and stability coefficient. On the basis of the obtained numerical results, the influences of axial force, P-Δ effect, and a vertical earthquake on the structural response are reviewed and their relative contribution is assessed. In addition, the applicability of the capacity-demand diagram method in seismic design of RC structures is reviewed by comparing the results obtained from the introduced method with those from rigorous nonlinear dynamic analyses.

KEY WORDS

dynamic P-Δ effect, RC columns, layered section method, vertical earthquake.

INTRODUCTION

When columns are subjected to cyclic loading such as earthquake loading, cracks occur over the length of the column from the bottom end. Increment of nonlinearity due to repetition of crack opening and closing may amplify the P-Δ effect. Many studies pertaining to the seismic P-Δ effect of slender columns have been conducted based on assumed hysteretic models such as the bilinear model and the stiffness degradation model.

Bernal (1987) characterized the effect of P-Δ on elastic-perfectly plastic oscillators by an amplification factor, which is defined as the ratio of the maximum acceleration sustained in a structure when the P-Δ effect is included divided by the corresponding value when the P-Δ effect is not included. Four ground motions were used and the ductility factor was held constant for each response spectrum. The amplification factor was characterized by a stability coefficient and ductility with high correlation, while there was no significant correlation between the structural period and the amplification factor. MacRae (1994) carried out nonlinear dynamic analyses using bilinear oscillators with different stiffness ratios and

---

[1] Professor, Civil and Envir. Engrg. Department, KAIST, 373-1 Guseong-dong Yuseong-gu Daejeon 305-701, KOREA, Phone +82 42/869-3621, FAX +82 42/869-3610, khg@kaist.ac.kr
[2] Researcher, Civil and Envir. Engrg. Department, KAIST, 373-1 Guseong-dong Yuseong-gu Daejeon 305-701, KOREA, Phone +82 42/869-3661, FAX +82 42/869-3610, glory@kaist.ac.kr

found that the increase in displacement or decrease in strength due to P-Δ become weak as the stiffness ratio was increased up to 0.25. His results agreed with those of Bernal, i.e., the correlation between the P-Δ effect and the structural period is very weak. An extensive series of analyses was performed on SDOF systems by Tremblay et al. (1997) in an effort to better understand the effects of the hysteretic models (bilinear, bilinear with slackness, and stiffness degradation models), the frequency content of earthquake ground motions (high frequency, moderated frequency, and low frequency), and the structural period (0.1-3.0s) of vibration on the P-Δ strength amplification factors. They found that the three factors noted above significantly influence the strength amplification factor and, more importantly, their effects appear to be interrelated. The bilinear with slackness and the stiffness degradation hysteretic models generally require a lower strength amplification factor to counteract the P-Δ effect than the standard bilinear hysteretic models with or without strain hardening. Although the P-Δ effect appears significant in conjunction with the structural period when subjected to low frequency ground motions, the capacity to correlate the effect of the structural period with the effect of the frequency contents of earthquakes is limited.

Williamson (2003) reviewed the effect of vertical earthquakes on the P-Δ effect on the basis of nonlinear dynamic analyses using the bilinear model and found that a vertical earthquake does not largely influence the seismic behavior of slender columns. However, according to Button et al. (2002), Ju et al. (2000), and Saadeghvaziri et al. (1991), buildings as well as bridges can be damaged by vertical earthquakes.

Different results may be obtained according to the assumptions employed for the curve, especially in RC structures where the behaviors are easily affected by axial force. However, since previous studies analyzed the seismic P-Δ effect based on the bilinear model or the stiffness degradation model, their results may not be directly applied to RC structures. Moreover, consideration of a vertical earthquake possibly affects the P-Δ effect as well as the load-displacement curve due to variation of axial force in an element, and this may lead to unacceptably discrepant results. Therefore, to review the P-Δ effect of slender RC columns under a seismic load, nonlinear dynamic analyses of slender RC columns are conducted with sixty sets of horizontal and vertical earthquake inputs based on the layered section approach. The numerical model can simulate the nonlinear behavior of slender RC columns under a seismic load considering the change of the load-displacement curve of a RC column due to an axial force. With the analysis results, the effects of axial force, P-Δ, and a vertical earthquake on the structural response are assessed.

MATERIAL MODEL

CONCRETE

Among the numerous mathematical models currently used in the analysis of RC structures, the monotonic envelope curve introduced by Kent and Park (1972) and later extended by Scott et al. (1982) is adopted in this paper because of its simplicity and computational efficiency. In this model, as shown in Fig. 3(a), the monotonic concrete stress-strain relation in compression is described by three regions, where ε_{co} is the concrete strain at maximum stress, K is a factor which accounts for the strength increase due to confinement, and Z is the strain softening slope.

It is assumed that concrete is linearly elastic in the tension region. Beyond the tensile strength, the tensile stress decreases linearly with increasing principal tensile strain. Ultimate failure from cracking is assumed to occur when the principal tensile strain exceeds the value $\varepsilon_{ut} = 2 \cdot G_f / f_t' \cdot ln(3/b)/(3-b)$, where b denotes the element length used in the finite element analysis and G_f is the fracture energy that is dissipated in the formation of a crack of unit length per unit thickness and is considered a material property. The value of ε_{ut} is derived from the fracture mechanics concept by equating the crack energy release with the fracture toughness of concrete G_f. An experimental study by Welch and Haismen (1969) indicates that for normal strength concrete the value of G_f / f_t' is in the range of 0.005~0.01 *mm*. If G_f and f_t' are known from measurements, then ε_{ut} can be determined.

The hysteretic rule for concrete proposed by Karsan and Jirsa is used. In addition, the unloading-reloading branches that always pass the origin regardless of the loading history are assumed in the tension region, because application of the introduced numerical model is limited to RC frame structures.

STEEL

Determination of element stiffness on the basis of the yielding of steel at a cracked section where a local stress concentration appears in the steel may result in overestimation of the structural response at the post-yielding range. Since this phenomenon is accelerated with increased deformation, an analysis of RC members subject to cyclic loading accompanying relatively large deformations requires the use of average stress-strain relations (Stevens et al. 1991, Belarbi et al. 1994). Accordingly, the average stress-strain relation of steel needs to be defined so as to trace the cracking behavior of RC beams and/or columns up to the ultimate limit state. The linear average stress-strain relation, which was introduced by Belarbi et al. (1994) from experimental data, is used in this paper.

A procedure is additionally used to consider the bond-slip effect in the layered section approach. In the approach, the bond-slip effect along the reinforcing bar is quantified with the force equilibrium and compatibility condition at the post-cracking stage and its contribution is indirectly implemented into the stress-stain relation of reinforcing steel. Among a number of models developed to describe the cyclic stress-strain curve of reinforcing steel, the most commonly used approach is the Giuffré-Menegotto-Pinto (G-M-P) model, introduced by Pinto et el. (1970, 1973); this model is also adopted in this paper. More details on the stress-strain relation of steel can be found elsewhere (Kwak et al. 2005).

SOLUTION ALGORITHM

In order to analyze RC columns, a layered section approach based on the Euler beam theory was used in this study. In a typical Euler beam, it is usual to assume that plane sections remain plane to represent linearity in the strain distribution of any section at any loading history. In addition, the effects of shear deformation are not taken into consideration in simulating nonlinear behavior since the normal bending stresses reach a maximum at the extreme fibers, where the transverse shear stresses are at their lowest value, and reach a minimum at mid-depth of the beam, where the transverse shear stresses are highest. Thus, the

interaction between transverse shear stresses and normal bending stresses is relatively small and can be ignored.

The time history analysis of the structure is based on the average acceleration method, which is one of two special cases in Newmark´s method because it does not require iteration to solve the equation of motion. More details can be found in reference (Chopra 1995).

DEFINITION OF STABILITY COEFFICIENT

In this study, the single degree of freedom (SDOF) system is considered. The load-displacement curve depends on the relative displacement, Δ, and is affected by the gravity load P. From the simple static consideration of the equilibrium condition for the system, the equation $V \cdot L + P \cdot \Delta = K_0 \cdot \Delta \cdot L$ is obtained; this can be expressed in the form of Eq. (1). From the equation, it is found that both the stiffness and the yield strength of the structure are reduced by $(1-\theta)$, where θ is the stability coefficient. Design codes such as ASCE-7 and IBC (2002, 2003), define the stability coefficient as the ratio of the secondary moment ($P \cdot \Delta$) to the primary moment ($V \cdot L$); since V/Δ represents the stiffness, the stability coefficient defined in these design codes can be expressed as $P/K_0 L$.

$$V = (K_0 - P/L) \cdot \Delta = K_0(1-\theta) \cdot \Delta, \; where \; \theta = P/K_0 L \qquad (1)$$

According to the design codes, if the stability coefficient does not exceed 0.1 there is no need to take the P-Δ effect into consideration, while story drift should be multiplied by $[1.0/(1-\theta)]$ for $0.1<\theta\leq\theta_{max}$. If θ is greater than θ_{max}, the structure is potentially unstable and must be redesigned. θ_{max} is given by ASCE-7 and IBC as $\theta_{max}=0.5/(\beta C_d)\leq0.25$, where β is the ratio of shear demand to shear capacity for the story between levels. If β is not calculated, β is to be taken as equal to 1.0. Since a deformation amplification factor C_d of 2.5 is used for ordinary reinforced concrete moment frames and 1.25 for the system considered here, θ_{max} becomes 0.2 for ordinary reinforced concrete moment frames and 0.25 for a reinforced concrete column with an inverted pendulum system. Meanwhile, Bernal (1987) derived the equation $\mu\theta=0.4$, which provides the limitation of ductility and stability coefficient based on an elastic-perfectly plastic oscillator. θ_{max} is 0.2 when the design ductility is assumed to be 2.0 for the conservative consideration. Therefore, θ_{max} of 0.2 is assumed in this study.

NONLINEAR DYNAMIC ANALYSES OF SLENDER RC COLUMNS

RANGE OF ANALYSES

In order to better understand the seismic behavior of slender RC columns, analyses for the practical ranges of the slenderness ratio and stability coefficient are performed with various earthquake inputs. Slenderness ratios of 40, 60, and 80 are chosen for the analysis with stability coefficients from 0.025 to 0.2, which give structural periods from 0.55s to 2.2s. For computational convenience, the axial force ($P=mg$) is assumed to be determined from the mass (m) multiplied by the acceleration of gravity. Mass is used for the computation of the stability coefficient ($\theta = P/K_0 L = mg \cdot L^2/3EI$) and the structural period ($T = 2\pi\sqrt{m/K_0} = 2\pi\sqrt{\theta L/g}$). Since there is a limitation to estimate the exact stiffness of a RC

structure due to the occurrence of cracks, the structural period is calculated based on the uncracked section. A *h=0.5m* square concrete column section with a 2% steel ratio, reinforced symmetrically by steel at 0.1*h* distance from each of the two critical faces, is used. The following material properties are assumed: f_c'=30 *MPa*, E_s=2.0×10⁵ *MPa* and f_y=400 *MPa*. The transfer length and the equivalent elastic modulus of steel determined on the basis of the procedure proposed in reference 1 are 0.884*m* and 1.28×10⁵ *MPa*, respectively.

Table 1: Analysis Variables

Period(s)	*kL/r*	*L (m)*	*Θ*	*P (kN)*	*P/P*$_{cr}$[1]	*P/P*$_u$[2]
0.55	40	3.0	0.025	558.9	0.030	0.067
0.78	40	3.0	0.050	1117.7	0.061	0.133
0.95	40	3.0	0.075	1676.6	0.091	0.200
1.10	40	3.0	0.100	2235.4	0.122	0.267
1.35	40	3.0	0.150	3353.2	0.183	0.400
1.55	40	3.0	0.200	4470.9	0.243	0.534
1.35	60	4.5	0.100	993.5	0.122	0.119
1.65	60	4.5	0.150	1490.3	0.183	0.178
1.90	60	4.5	0.200	1987.1	0.243	0.237
1.55	80	6.0	0.100	558.9	0.122	0.067
1.90	80	6.0	0.150	838.3	0.183	0.100
2.20	80	6.0	0.200	1117.7	0.243	0.133
[1]$P_{cr} = \pi^2 EI(kL)^2$ (ACI 318-02 2002); [2]$P_u = 0.85f_{ck}A_c+f_yA_s$						

Periods and axial forces for RC columns with slenderness ratios of 40~80 are listed in Table 1 and the axial force for each stability coefficient is marked in the P-M interaction diagram in Figure 1. As shown in Figure 1, when the slenderness ratio is 40, the ratios of axial forces (*P*) to the ultimate section resistance (P_u) are 27-53% for stability coefficients from 0.1 to 0.2, and 7-24% in the cases of *L/r*=60 or 80. Since the energy absorption capacity and the ductility of a RC column decrease steeply when the axial force increases up to the balanced axial load, most RC columns are designed to resist axial forces less than the balanced loads. Therefore, the case where the axial force is relatively high, i.e., a slenderness ratio of 40 and a stability coefficient of 0.2, is excluded from the analysis. However, stability coefficients from 0.025 to 0.075 are additionally considered for comparison with the cases of slenderness ratios of 60 and 80, whereby the axial forces for the stability coefficients of 0.1~0.2 are relatively small. When the slenderness ratio is 40, P/P_u is larger than P/P_{cr} in contrast to the cases where the slenderness ratio is 60 or 80. This means that a column with a slenderness ratio of 40 is governed by material nonlinear behavior rather than geometric nonlinearity. Therefore,

different behaviors according to the stability coefficient are expected compared with other slender columns.
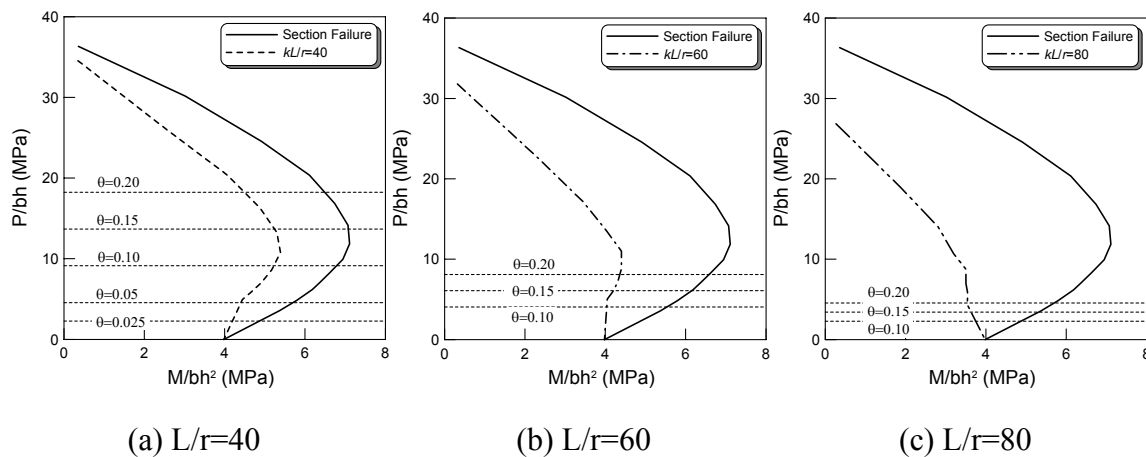

(a) L/r=40   (b) L/r=60   (c) L/r=80

Figure 1 Axial forces according to stability coefficients

Since the nonlinear dynamic behavior of a structure depends on the characteristics of the earthquake (Tremblay 1997, Williamson 2003), sixty sets of horizontal/vertical earthquake inputs collected from the PEER Strong Motion Database (http://peer.berkeley.edu/smcat/), chosen for their value in an engineering analysis, are used. All the earthquake inputs are uniformly distributed from 0.01g to 0.6g. According to previous studies by Button et al. (2002) and Ju et al. (2000), the effect of a vertical earthquake becomes dominant when the vertical component of the earthquake is not small compared with the horizontal component. Among the 60 earthquake inputs the number of inputs where vertical-to-horizontal ratio (V/H) is larger than 0.7 is 21 while five inputs have V/H ratios larger than 1.0. Thus, the inputs may be effectively used to assess the effect of a vertical earthquake. All earthquake inputs are processed to make the data useful for an engineering analysis: (1) correction for the response of the strong motion instrument

ANALYSES RESULTS

The current seismic design concept has shifted toward a performance-based design from the previous force-based design, and thus deformation rather than force will be useful in estimating a structure's performance. In this study, maximum rotation ($\alpha=u_m/L$, *radian*) is chosen for reviewing the nonlinear dynamic behavior of slender RC columns. To take a closer look into the effect of axial force, P-Δ effect, and a vertical earthquake, the following four cases are analyzed for each earthquake input: (1) Consideration of mass only with no consideration of axial force similar to previous studies based on the assumed load-displacement curve for a horizontal earthquake (hor0); (2) Consideration of mass and axial force but not P-Δ effect for a horizontal earthquake (hor1); (3) Consideration of mass and axial force including P-Δ effect for a horizontal earthquake (hor01g); and (4) Consideration of mass and axial force including P-Δ effect for earthquakes including horizontal and vertical components (hor/ver01g).

For a slenderness ratio of 40, Figure 2(a), (c) (hor0-hor01g, hor0-hor/ver01g) present the results of case (1) for the x-axis and case (3) or (4) for the y-axis, and Figure 2(b), (d) (hor1-hor01g, hor1-hor/ver01g) present the results of case (2) for the x-axis and case (3) or (4) for the y-axis. As shown in Figure 2, the results obtained with no consideration of the P-Δ effect are linearly correlated to the results obtained by considering the P-Δ effect with a high correlation coefficient R^2 of 0.85-0.99. The linear regression formulas are noted in the figures. Assessment of the results is made by comparing the slopes of the regression formulas. When the results of hor0 are presented in the x-axis (hor0-hor01g, hor0-hor/ver01g), the slopes range from 0.86 to 0.93 less than 1.0. That is, the rotation of an RC column decreases by 7~14% due to axial force or P-Δ effect relative to the results of hor0. Note that the increment of stiffness, yield strength, and pinching phenomena due to axial force dominantly reduce the seismic behavior for a column with a slenderness ratio of 40, even though the P-Δ effect generally leads to increased deformation. Meanwhile, when the results of hor1 are presented in the x-axis, hor1-hor01g, hor1-hor/ver01g, which isolate the effects of P-Δ and the vertical earthquake from the effect of axial force, the slopes range from 1.03 to 1.04, i.e., larger than 1.0. That is, the effects of P-Δ and the vertical earthquake result in increased rotation, but the increase is negligibly small.
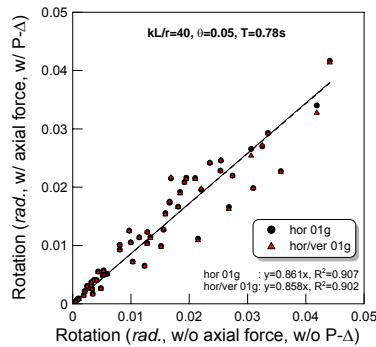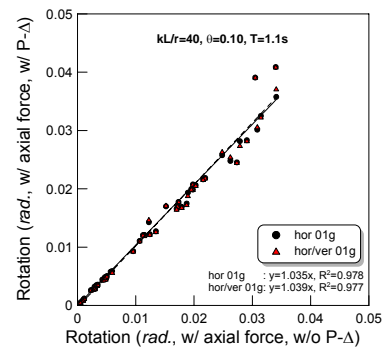

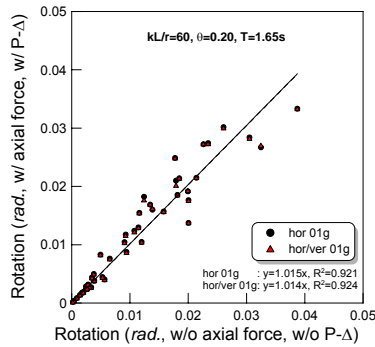(a) L/r=40, θ=0.05 (x-axis: hor0)
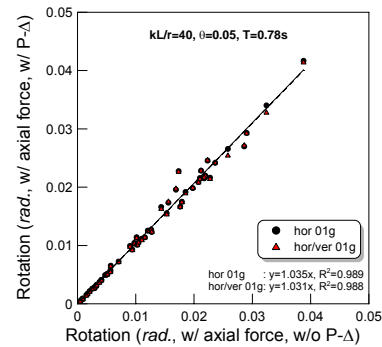
(b) L/r=40, θ=0.05 (x-axis: hor1)
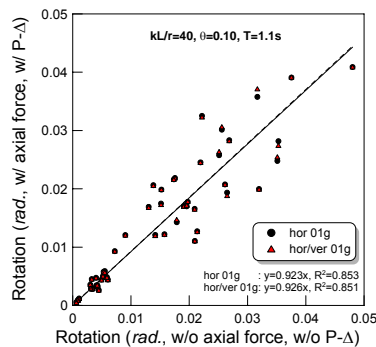
(c) L/r=40, θ=0.10 (x-axis: hor0)
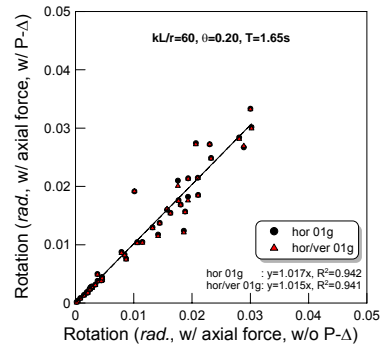
(d) L/r=40, θ=0.10 (x-axis: hor1)

Figure 2 Seismic P-Δ Effect when L/r=40

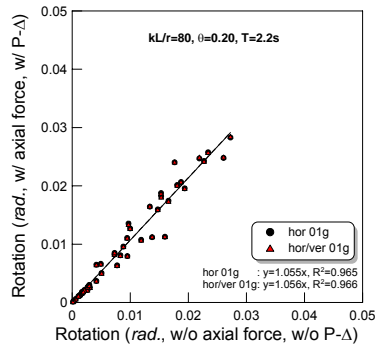(a) L/r=60, θ=0.20 (x-axis: hor0) (b) L/r=60, θ=0.20 (x-axis: hor1)
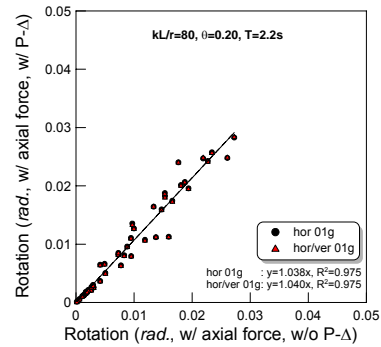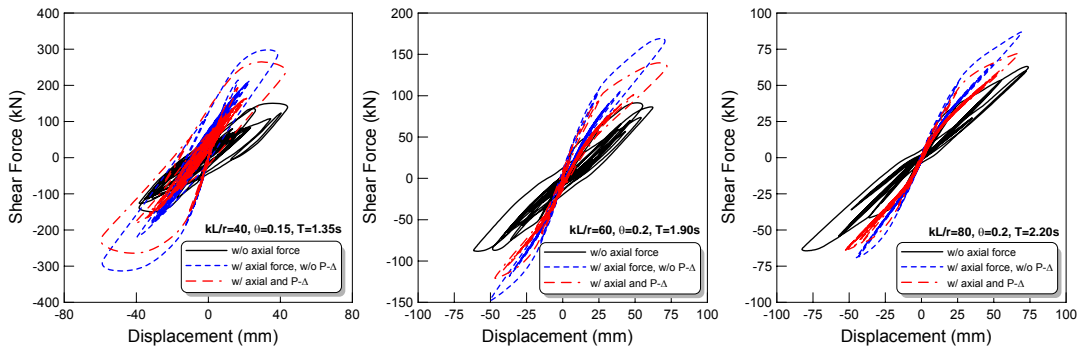
Figure 3 Seismic P-Δ Effect when L/r=60

(a) L/r=80, θ=0.20 (x-axis: hor0) (b) L/r=80, θ=0.20 (x-axis: hor1)

Figure 4 Seismic P-Δ Effect when L/r=80

(a) L/r=40, θ=0.15   (b) L/r=60, θ=0.20   (c) L/r=80, θ=0.20

Figure 5 Load-Displacement Curves (input: 46314 Cantua Creek School 1983)

The results of columns with slenderness ratios of 60 and 80 are shown in Figure 3 and 5.
When hor0 and hor1 is the x-axis, slopes of the figures range from 1.02~1.06 and 1.02~1.04,
respectively. Similar to the case when the slenderness ratio is 40, the effects of P-Δ and the

vertical earthquake are small. However, in this case, the effect of axial force appears to be negligible, as the difference in the slopes noted above is very small. Comparing Figure 2 with Figure 3 and 5, rotation (*radian*) is larger when slenderness ratio is 40. This means that more plastic behavior appears in shorter columns even though larger deformation is shown in longer columns (see Figure 5). Axial forces for the same stability coefficient differ according to the slenderness ratio, and the axial forces are small in columns with a larger slenderness ratio. Thus, the increment of stiffness, yield strength, and pinching phenomena is less than those in relatively smaller columns and the parameters have less impact on the structural behavior in longer columns. Furthermore, structures with large structural periods are less sensitive to a change of period than the structures with a small structural period. For these reasons, the columns with slenderness ratios of 60 and 80 are relatively uninfluenced by axial force and P-Δ effect.

In order to define the overall trend of the obtained results the slopes of the regression formulas for each set of slenderness ratio and stability coefficient are listed in Table 2. For the case of hor0-hor1 in Table 2, the slopes range from 0.83 to 0.89 when the slenderness ratio is 40 with stability coefficients of 0.025~0.10. This reflects that the effect of axial force reduces rotation. When the slenderness ratio is 40 with stability coefficients of 0.15, the slope is 0.99. This is attributed to the axial force being larger than the balanced load (P_b) (see Figure 1): this increases nonlinearity in a section and changes tension-controlled section behavior to compression-controlled section behavior, consequently reducing cracks and pinching phenomena (see Figure 5). When the slenderness ratio is 60 or 80, all the slopes are close to 1.0. This may be because columns with high slenderness ratios are rarely affected by axial force, as noted above.

Table 2: The Effects of Axial Force and Seismic P-Δ

Period(s)	*kL/r*	*θ*	hor0-hor01g	hor0-hor/ver01g	hor1-hor01g	hor1-hor/ver01g	hor0-hor1
0.55	40	0.025	0.903	0.910	1.028	1.037	0.878
0.78	40	0.050	0.861	0.858	1.035	1.031	0.832
0.95	40	0.075	0.924	0.924	1.046	1.046	0.883
1.10	40	0.100	0.923	0.926	1.035	1.039	0.891
1.35	40	0.150	1.026	0.999	1.034	1.027	0.992
1.35	60	0.100	1.000	1.001	1.040	1.042	0.961
1.65	60	0.150	0.990	0.996	0.997	1.004	0.993
1.90	60	0.200	1.015	1.014	1.017	1.015	0.998
1.55	80	0.100	0.980	0.979	0.997	0.996	0.983
1.90	80	0.150	0.979	0.981	1.018	1.020	0.962
2.20	80	0.200	1.005	1.055	1.056	1.038	1.016

Through the results of hor1-hor01g in Table 2, the isolated effect of P-Δ can be reviewed. All the results of hor1-hor01g show that the increment of rotation by the P-Δ effect is less than 6%. The effect of a vertical earthquake can be investigated by comparing hor1-hor01g with hor1-hor/ver01g. As shown in Table 2, the difference between the two cases is very small, i.e., within 2%, and thus the effect of the vertical earthquake may be negligible. The results of hor0-hor01g and hor0-hor/ver01g show the effect of axial force, P-Δ, and a vertical earthquake simultaneously compared with the case where axial force is not considered (hor0). When the slenderness ratio is 40 and the stability coefficients ranges from 0.025~0.10, the results show that the rotation decreases by more than 8% as a result of the effect of axial force and P-Δ. Note that the effect of axial force dominantly reduces the rotation, thus mitigating any increase that would result from the P-Δ effect. However, in all other cases, since both the effects are very weak, all other results of hor0-hor01g and hor0-hor/ver01g are close to 1.0. Therefore, the effects of axial force, P-Δ, and a vertical earthquake on rotation ($\alpha = u_m/L$, *radian*) are acceptably negligible in the seismic design of slender RC columns. Meanwhile, as shown in Figure 5, since the increment of an internal force may appear when axial force is considered, additional consideration of the effect is required.

CONCLUSIONS

Unlike the previous studies which have investigated the seismic P-Δ effect of slender based on assumed hysteretic models such as the bilinear model and the stiffness degradation model, the approach adopted in this paper can simulate the change of the load-displacement curve of a RC column due to an axial force, especially in terms of stiffness, yield strength, and pinching phenomena. Through the results of numerical analyses, it is found that, in some cases, the effect of axial force dominantly reduces the rotation, thus mitigating any increase that would result from the P-Δ effect. However, in the most of other cases, the effects by axial force, P-Δ, and a vertical earthquake are very weak. Therefore, the effects of the parameters on rotation are acceptably negligible in the seismic design of slender RC columns. Meanwhile, since the increment of an internal force may appear when axial force is considered, additional consideration of the effect is required.

ACKNOWLEDGMENTS

REFERENCES

Kwak, H.G., Kim, J.K. (2005*). "Implementation of bond-slip effect in analyses of RC frames under cyclic loads using layered section method." *Engineering Structures*, Submitted

Bernal, D. (1987). "Amplification factors for nonlinear dynamic p-δ effects in earthquake analysis." *Earthquake Engineering and Structural Dynamics*, 15: 635-651.

Tremblay, R. (1997). "Effects of hysteretic models and ground motion characteristics on seismic p-delta strength amplification factors." *Stability and Ductility of Steel Structures*, SDSS 97: 311-318.